Strength of threaded connections additively produced from polymeric materials

Tomasz Dziubek[1] (ORCID ID: 0000-0002-3259-446X), **Grzegorz Budzik[1]** (0000-0003-3598-2860),
Andrzej Kawalec[1] (0000-0002-2120-8535), **Mariusz Dębski[1]** (0000-0002-4889-7633), **Paweł Turek[1]**
(0000-0002-5926-4815), **Mariusz Oleksy[2], *)** (0000-0001-5515-8575), **Andrzej Paszkiewicz[3]** (0000-0001-7573-3856),
Przemysław Poliński[4] (0000-0002-1052-644X), **Łukasz Kochmański[4]** (0000-0003-3635-3812),
Mateusz Kiełbicki[4] (0000-0002-8116-4589), **Jerzy Józwik[5]** (0000-0002-8845-0764), **Ivan Kuric[6]** (0000-0003-0267-786X),
Józef Cebulski[7] (0000-0001-5657-5354)

Abstract: The article presents the results of strength tests of screw-nut threaded connections made of polymeric materials such as: ABS, PLA, PET-G and acrylic resin. In order to make physical models, three 3D printing techniques were used: Fused Deposition Modeling (FDM), Fused Filament Fabrication (FFF), and PolyJet. The tests took into account the stresses caused by the axial force generated when the bolt is screwed into the nut or other structural element. Due to the complexity of the issue, the presented studies are only a starting point for further research.

Keywords: additive manufacturing; polymers; screw strength, tensile stresses, shear stresses.

Wytrzymałość połączeń gwintowych wytwarzanych przyrostowo z materiałów polimerowych

Streszczenie: W artykule przedstawiono wyniki badań wytrzymałości połączeń gwintowych śruba--nakrętka wykonanych z materiałów polimerowych takich, jak: ABS, PLA, PET-G i żywicy akrylowej. Do wykonania modeli fizycznych stosowano trzy techniki druku 3D: FDM, FFF i PolyJet. W badaniach uwzględniono naprężenia spowodowane działaniem siły osiowej powstającej podczas wkręcania śru-by w nakrętkę lub inny element konstrukcyjny. Ze względu na złożoność zagadnienia, przedstawione badania stanowią punkt wyjścia do dalszych badań.

Słowa kluczowe: wytwarzanie przyrostowe, polimery, wytrzymałość śruby, naprężenia rozciągające, naprężenia ścinające.

Traditional modeling of elements and machine parts is carried out using Computer-Aided Design (CAD) systems, which are now widely used in the design of industrial products [1]. It all starts with the constructor's idea. Then an element is modeled in a CAD system. They allow forming any geometry of models used in the automotive [7, 8], aviation [9, 10], and medical industries [11, 12]. Currently, many scientific publications present and test various types of gears manufactured with additive techniques [13–15]. However, there is a lack of comprehensive tests concerning, among other things, screw-threaded joint manufactured of polymeric materials. Screw threaded joints are significant. They are used primarily as movement connections in mechanisms that convert rotary into translational movement, *e.g.*, machine tool drives, presses, or lifts. Their goal is an effective and safe connection of elements with each other. Therefore they must guarantee a constant and high value of the clamping force while ensuring ease of disassembly [16, 17]. Calculating the strength of screw-threaded joint can be a long and complicated process. However, since the screw thread mechanisms are movable connections and can only be loaded with forces axi-

---

[1] Rzeszow University of Technology, Faculty of Mechanical Engineering and Aeronautics, 35-959 Rzeszow, Poland.

[2] Rzeszow University of Technology, Faculty of Chemistry, 35-959 Rzeszow, Poland.

[3] Rzeszow University of Technology, Faculty of Electrical and Computer Engineering, 35-959 Rzeszow, Poland.

[4] Rzeszow University of Technology, Doctoral School of Engineering and Technical Sciences, 35-959 Rzeszow, Poland.

[5] Faculty of Mechanical Engineering, Lublin University of Technology, 20-618 Lublin, Poland.

[6] University of Žilina, Faculty of Mechanical Engineering, Department of Automation and Production Systems, SK-010 26 Žilina, Slovak Republic.

[7] University of Rzeszow, Institute of Physics, 35-959 Rzeszow, Poland.

*) Author for correspondence: molek@prz.edu.pl

ally towards the bolt or with a torsional moment, it is crucial to calculate [18].

The manufacture of screw-threaded elements carried out with additive techniques is a new approach for obtaining this product. Presently, it is a niche approach to manufacturing temporary fastening elements, which is not a popular topic in the available literature. The scope and results of the research, if they are conducted, are not published. The same applies to the approach to the development of the 3D-CAD models geometry. In the 3D-CAD modeling process, it is necessary to determine the fitting value of the screw-threaded joint manufactured with additive techniques [19]. This complex issue cannot be directly implemented based on the guidelines provided for standard screw thread manufacturing procedures [20, 21]. In connection with the specificity of additive techniques, this relationship translates into preparing the appropriate geometry of the output models [22]. When models are made of polymeric materials, there are differences between the nominal 3D-CAD model and the manufactured product [23–25]. These differences result mainly from the subsequent hardening layers and the type of material used during 3D printing [26–28]. In addition, each 3D printer has specific characteristics and requirements concerning working conditions (environmental conditions, process temperature, model finishing treatment). The factors mentioned earlier influence dimensional and geometrical errors and changes in the values of surface roughness parameters [29–32]. Their determination is necessary in order to obtain an appropriate screw-threaded joint. Thanks to the development of modern measurement systems, it is possible to precisely verify the accuracy of the macro and micro geometry [33] and elements manufactured using additive techniques. Verification of the manufactured product is most often carried out using contact coordinate measuring systems [34–36]. There is also a rapid development of optical systems based on laser and structured light [37–39], industrial tomographic systems [26], and focus variation method [40].

Despite the variety and availability of many methods of designing and manufacturing screw-threaded joint, no research has been carried out on the most commonly used polymer materials in the 3D printing process. Additive processes allow almost any manufacturing of screw-threaded joint elements. However, it requires knowledge of the geometrical relationships of a thread itself and the strength of materials from which the screw-threaded joint is made. There is a noticeable lack of detailed information relating to the torsional strength of additive-processed polymeric materials. The article presents the results of the screw thread-nut M24 screw-threaded elements with a pitch of 3, manufactured of polymeric materials using PolyJet, FDM, and FFF technologies. The elements of the screw-threaded joints were also tested for static torsional strength using a unique test stand.

EXPERIMENTAL PART

Materials and methods

Design research models

In this study, as a research model, the M24 screw thread-nut pair was designed with the nominal geometry and with the allowance values for two selected values [41], which were included in the nut models. The diametrical parameters of the screw threads were adopted as nominal for all its configurations, and only the active screw thread length along with the length of the pin were modified. In addition, for two screw thread variants, an additional bearing surface was introduced, blocking the rotation of the nut in a selected range during bench tests.

The modeling process, both for the screw thread and the nut, was carried out using solid modeling based on the preparation of a screw thread outline by dragging the profile along a helix [41]. Its geometry has been taken into account here, ensuring that the cutting profile exits the material at the end of the screw thread. The developed model was subjected to the parameterization process [41]. For the presented dependencies, respectively, nominal screw thread models with a pin length of 50 mm with a bearing surface (Fig. 1a), 100 mm long without a bearing surface, and 100 mm long with a bearing surface were created and tessellated.

As a cooperating element, adopting the modeling methodology analogous to the thread, the CAD model of the nut was developed in three versions. However, in this case, the geometry of parts has been modified concerning the nominal value by assumed clearance values. For this purpose, the cutting profile was shifted by 0.25 mm and 0.5 mm in the direction normal to the nut axis, and the internal thread diameter was increased by identical values. The other parameters remained unchanged. The models developed for production with the use of additive techniques were subjected to a tessellation process (Fig. 1b).

The adopted values of parameters describing the geometry of 3D-CAD models were selected based on experience resulting from many years of practice in manufacturing with additive techniques and technical data defining the accuracy of the used devices. The developed geometry of the numerical models took into account the specific methodology of the screw thread modeling process, which cannot be directly implemented from the

Fig. 1. The nominal models: a) screw thread with a bearing surface, b) nut

T a b l e 1. **The additive manufacturing techniques and materials used**

AM processes	AM technology	3D Printer	Polymer	Trade name	Producer	Layer thickness	State
Extrusion	FDM	Stratasys F170	Acrylonitrile butadiene styrene copolymer	ABS-M30	Stratasys (USA)	0.177 mm	Solid
	FFF	Prusa MK3s	Polylactic acid	PLA	Prusa Research (Czech Republic)	0.150 mm	
			Acrylonitrile butadiene styrene copolymer	ABS			
			Glycolized polyester	PET-G			
Jetting	MJ	Objet Eden 260	Acrylic resin	RGD720	Stratasys (USA)	0.016 mm	Liquid

standard parameters of the screw thread resulting from its accuracy class related to screw threaded joint produced with the use of CNC methods [20, 22]. Based on the 3D-CAD models of the screw thread-nut pair geometry prepared in the presented manner, producing physical research models was carried out using selected additive techniques.

Manufacture research models using additive techniques

In order to make physical models, three 3D printing techniques were used: Fused Deposition Modeling (FDM), Fused Filament Fabrication (FFF), and PolyJet (Tab. 1).

Manufacturing a model using the FFF and FDM method consists in melting the material (filament) in a heated head, and then putting it on the worktable [26, 27]. The 3D printing process of models using the FFF technique was carried out on a Prusa MK3s printer. Three types of polymer materials were used: PLA (Fig. 2a), ABS (Fig. 2b), and PET-G (Fig. 2c).

PLA is a biopolymer classified as an aliphatic polyester. This material is characterized by quite good tensile strength and stiffness. ABS is a material obtained in butadiene polymerization and copolymerization of acrylonitrile with styrene with simultaneous grafting of the resulting copolymer on polybutadiene. Compared to PLA, it has better hardness, impact, and abrasion resistance and good tolerance of high temperatures, because it retains its properties in the temperature range from -20 to 80°C. However, it is not resistant to ultraviolet rays. It crumbles after prolonged exposure to sunlight. It is also less stiff and more susceptible to shrinkage than PLA. PET-G combines the properties of both PLA and ABS, which means that it is relatively easy to print, and at the same time, mechanically strong. The softening point of PET-G is around 80–85°C, so it is not as high

a)   b)   c)
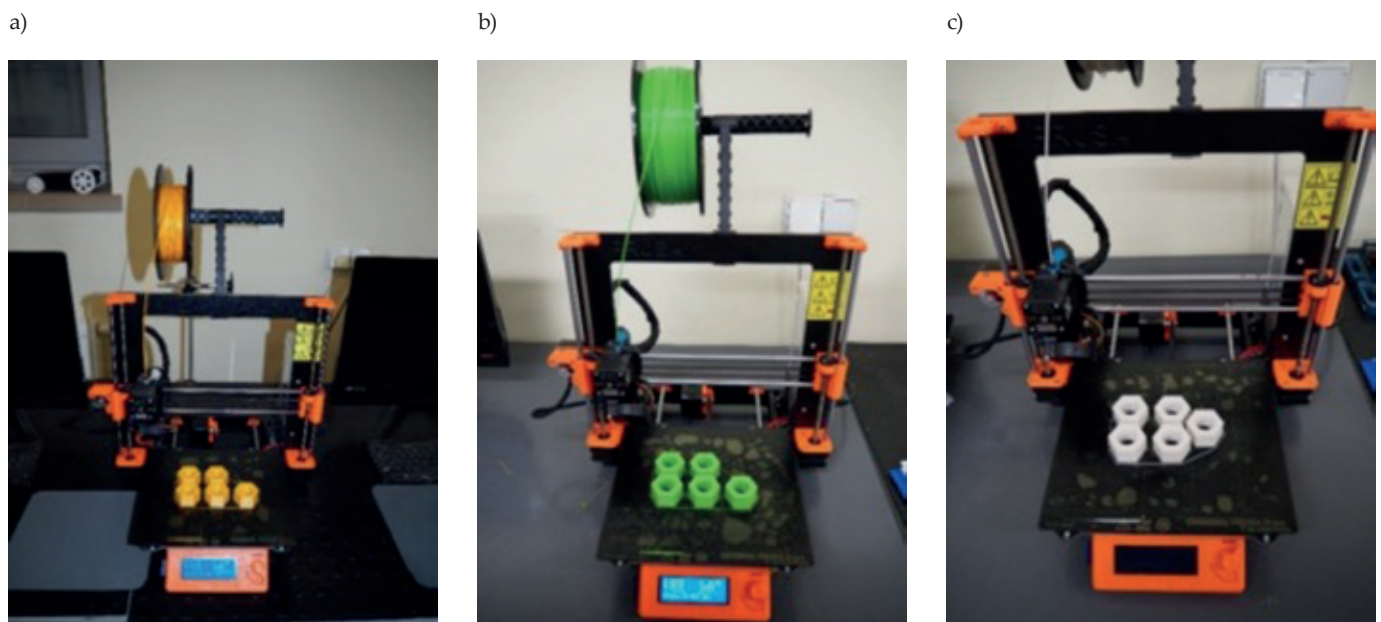
Fig. 2. The process of 3D printing nut models using the FFF technique: a) PLA, b) ABS, c) PET-G
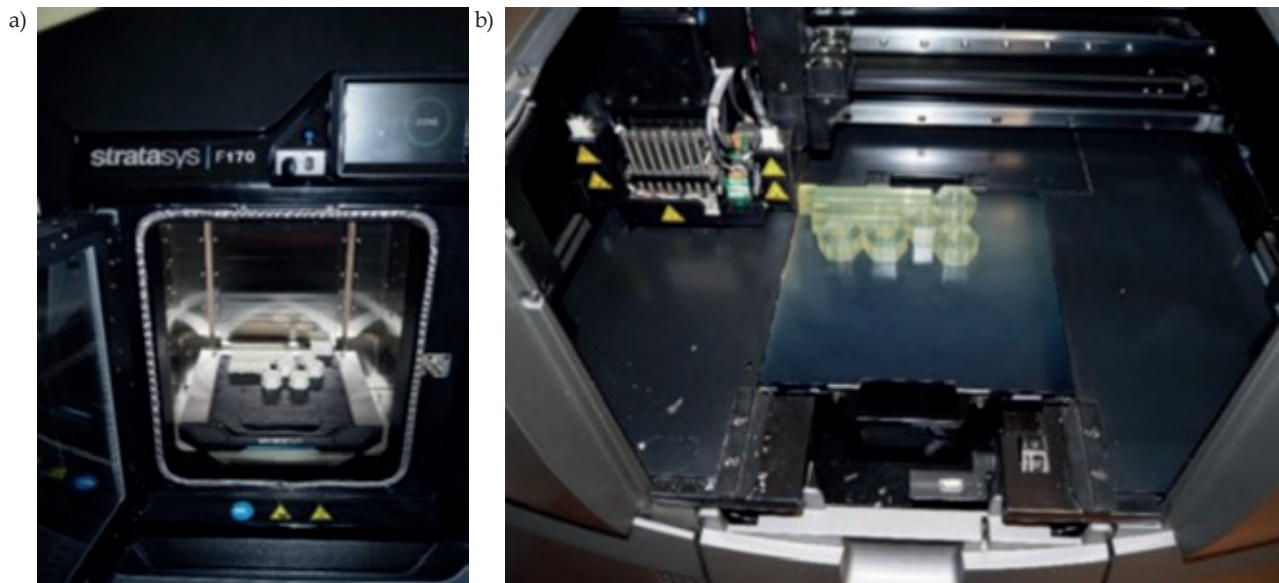
a) b)

Fig. 3. Manufacturing models using the FDM and PolyJet techniques: a) Stratasys F170, b) Objet Eden 260 printer

as in ABS but much higher than in PLA. So it can be said that PET-G can work at elevated temperatures [51, 52].

The model printing process was carried out on a Stratasys F170 printer (Fig. 3a) using the FDM technique. ABS-M30 was used in the printing process. The ABS-M30 retains all the advantages of standard ABS but has an increased level of strength ranging from 25% to 70%. Using the PolyJet technique, thin layers of acrylic resin were applied, which were hardened on an ongoing basis (immediately after application) by irradiation with an ultraviolet lamp (the so-called polymerization process) [26, 35]. The process using the PolyJet technique was carried out on the Objet Eden 260 printer (Fig. 3b).

The RGD720 was used in the printing process of the models. RGD720 is a universal photopolymer resin that enables the creation of functional prototypes and parts for fit tests. This stiff material is perfect for conceptual modeling. This material provides high dimensional sta-

bility and surface smoothness. As a result, models of screw threads and nuts (Fig. 4) were subjected to macro and micro geometry tests and static torsional strength using a unique test stand.

Screw strenght – analitical models. Static torsional strength analysis using a unique test stand

The axial force F_Q acting in the bolt is transmitted through the bolt core and the threads. This force causes the following conditions: compression or tension of the bolt core, bending and shearing of the threads, and pressure on the thread surface. As a rule, for standard threads, taking into account the small overhang of loads distributed over the contact surfaces of the thread, the bending strength of the threads is significantly greater than other types of the threads strenght. Therefore, the strength of the bolt core and the shear strength of the thread as well as the pressure on its surface are usually

Fig. 4. Final research models

considered to be the most important and decisive for the strength of the bolt. Hence, the following strength criteria are assumed, related to: stretching of the bolt core (1), shear of the thread (2) and surface pressure on the thread turns (3) [44-46]:

$$\sigma_C = \frac{F_Q}{A_C} \leqslant k_C \qquad (1)$$

$$\tau_T = \frac{F_Q}{A_T} \leqslant k_T \qquad (2)$$

$$p = \frac{F_Q}{A_p} \leqslant p_A \qquad (3)$$

where: σ_C, τ_T, p – tensile stresses in the bolt core, shear stresses in the cross section of the thread, surface pressures on the thread surface, respectively; k_C, k_T and p_A – allowable magnitudes of tensile stress, shear stress and pressures, respectively; A_C, A_T and A_p – tension area of the bolt core, area of the thread turns under shear, contact area of the threads, respectively.

Therefore, damage to the bolt will occur when the permissible stresses are exceeded, which for the above-mentioned load forms are expressed by the following conditions:

$$F_{QCA} = k_C A_C \qquad (4)$$

$$F_{QTA} = k_T A_T \qquad (5)$$

$$F_{QpA} = p_A A_p \qquad (6)$$

where: F_{QCA}, F_{QTA} and F_{QpA} – permissible loads resulting from the conditions (4), (5) and (6), respectively.

The tension area A_C of the bolt core can be calculated as for a wheel, taking into account the bolt core diameter d_C. The surface areas A_T, A_p are calculated assuming that the shape and dimensions of the bolt and thread are perfectly consistent with the nominal and that all thread turns evenly transmit the axial force F_Q:

$$A_C = \frac{\pi d_C^2}{4} \qquad (7)$$

$$A_T = \pi d_T h_T n = \frac{\pi d_T h_T N}{P} \qquad (8)$$

$$A_p = \frac{\pi(d_z^2 - D_w^2)n}{4} = \frac{\pi(d_z^2 - D_w^2)N}{4} \qquad (9)$$

where: n – number of thread turns in use, N – the height of a nut or the length of the screw that is screwed into another element, P – thread pitch, d_T – diameter where the thread was cut, h_T – height of the thread turn section at d_T, d_z – outer diameter of the screw thread, D_w – inside diameter of the nut thread. In the case of metric thread, the following relationships apply between the geometric quantities describing the bolt and its thread, *i.e.* the ISO metric screw thread [20, 22, 46, 47]:

$$H = \frac{P}{2\tan 30°} = 8.66P, \quad t = \frac{5H}{8} \qquad (10)$$

$$d_1 = d - 2t, \quad d_3 \cong d - 1.316P \qquad (11)$$

Allowable bolt load resulting from tension in the bolt core takes into account that the core diameter $d_C = d_3$. Therefore, the area A_C used in eq. (7) can be expressed as:

$$A_C \cong 0.25\pi(d - 1.316P)^2 \qquad (12)$$

That leads to permissible loads resulting from the condition defined by eq. (4):

$$F_{QCA} = 0.25\pi(d - 1.316P)^2 k_C \qquad (13)$$

Allowable bolt load resulting from shear condition of the thread turns takes into account that the thread is sheared on the diameter d_t along the length h_t. The permissible shear forces in the bolt and nut can be calculated as the product of the appropriate coefficient of the share coefficient of the shear height of the bolt threads c_b and nut c_n in the thread pitch P and the shear strength k_{Tb} of the bolt material and the nut material k_{Tn}. Taking into account the balance of shear forces in the bolt and nut, the participation factors can be calculated [47]:

$$c_b = \frac{k_{Tn}}{k_{Tb} + k_{Tn}} \qquad (14)$$

$$c_n = \frac{k_{Tb}}{k_{Tb} + k_{Tn}} \qquad (15)$$

Taking into account the geometric features of the metric thread [20, 22, 46, 47], it is possible to obtain formulas defining the diameter d_t and the height h_t, which are included in the formula for the area A_T used in eq. (8) and next in eq. (5) for the permissible load resulting from the condition of the permissible shear stresses in the cross section of the thread [47]:

$$d_t = d\left[1 - \left(0.65 - \frac{2c_n - 1}{2\tan 30°}\right) - \frac{P}{d}\right] \qquad (16)$$

$$h_t = c_n P \qquad (17)$$

The permissible bolt load due to surface pressures takes into account the contact area of the thread turns of the bolt and the nut metric thread. This field can be expressed by the formula:

$$A_p = \frac{\pi n\left(d^2 - D_1^2\right)}{4} \qquad (18)$$

where: D_1 denotes the inner diameter of the nut thread. This diameter can be expressed for the metric thread using the outer diameter of the screw thread $d = d_z$ and the height of thread H defined by eq. (10) [20, 22, 47]:

$$D_1 = d - \frac{5}{4}H \qquad (19)$$

From eq. (18), (19) and (20) it follows

$$d^2 - D^2 = 2.5H\left(d - \frac{5}{8}H\right) = 2.165P(d - 0.5413P) \quad (20)$$

Therefore, the contact area A_p of the thread turns of the bolt and the nut metric thread can be calculated according to the following formula:

$$A_P = \frac{2.165P(d - 0.5413P)\pi N}{4P} \qquad (21)$$

Finally, the permissible load resulting from the condition of permissible surface pressures between the bolt and nut threads, determined by conditions defined with eqs. (3) and (6), can be expressed by the following formula:

$$F_{QpA} = \frac{2.165P(d - 0.5413P)\pi N p_A}{4P} \qquad (22)$$

In the case of a metric thread, the permissible loads F_{QCA}, F_{QTA} and F_{QpA} are determined by the formula (13) for the permissible tensile stresses in the bolt core, by the formulas (5), (8), (16), (17) for the permissible shear stresses in the cross section of the thread and by the formula (22) for the permissible surface pressures on the thread surface, respectively.

The analysis of the calculation results according to the above formulas for specific materials and their properties as well as the basic geometric characteristics of a metric thread will allow to estimate which of the conditions (1), (2) or (3) leads to the smallest axial load, defined by eqs. (4), (5) and (6), respectively, that can damage the bolt or thread core. In the case of screws made of polymer materials with additive techniques, other factors that may have a negative effect on the strength of the screw or thread must be taken into account. These include the natural discontinuity of the bolt material, resulting from micropores or the adoption of light internal structures, e.g. using different hatch patterns or scanning strategies, as well as the impact of the friction process on the bolt and nut threads surface including the heat generated in this process.

In the presented studies, the static torsion test was determined based on the constructed test stand (Fig. 5).

The stand is equipped with a motor, transmission system, control system, torque sensor and motion control (encoder), measuring system, and results recorder connected to a computer. The torque is forced using an electric motor and worm gears with a total gear ratio of 1: 1800. The recording of the test results is carried out by a static torque sensor connected to the Mecmesin AFTI 17-0135-1 recorder and proprietary software recording the results in real-time. The obtained software data allow obtaining results in the torque value as a function of the angular displacement. The force is carried out with the assumed rotational speed of 0.5 rpm.

RESULTS

Based on the prepared test stands, results were obtained to assess the accuracy of the model geometry and the static torsional strength. The results are presented in Table 2 and Figures 6–10 in the form of dependence curves of the torque versus the torsion angle for nominal screw thread models with a pin length of 50 mm. Additionally, Figures 6–10 present also the fracture surface morphology after the static torsion test at 10x magnification, performed using the KERN OZL-466 stereoscopic microscope and view of the sample after testing.
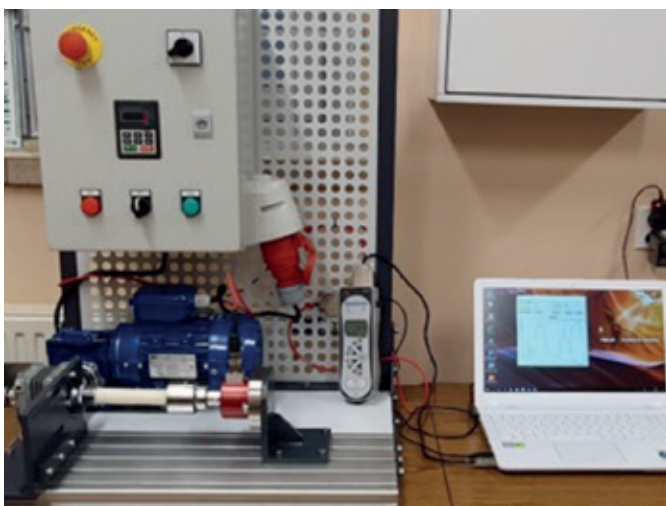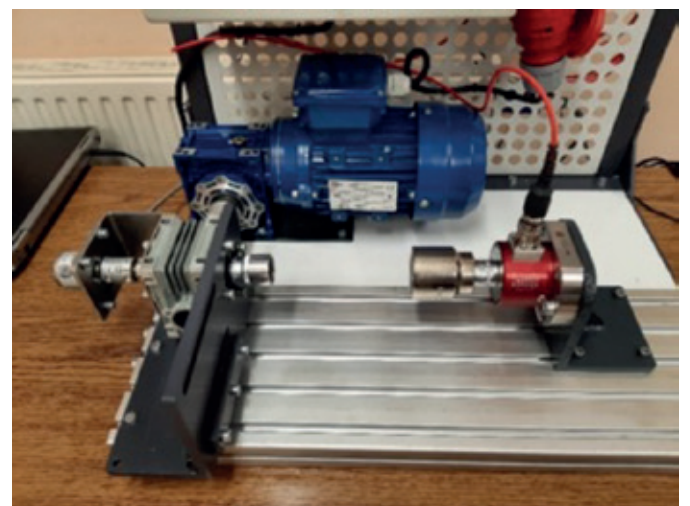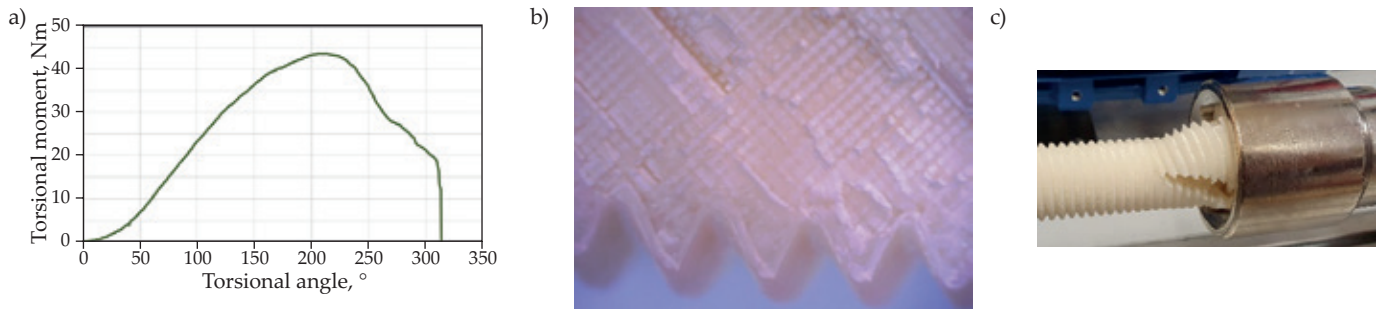

Fig. 5. Torsional strength test stand

F i g. 6. ABS-M30: a) torque vs. angle diagram, b) fracture surface morphology, c) view of the sample after testing
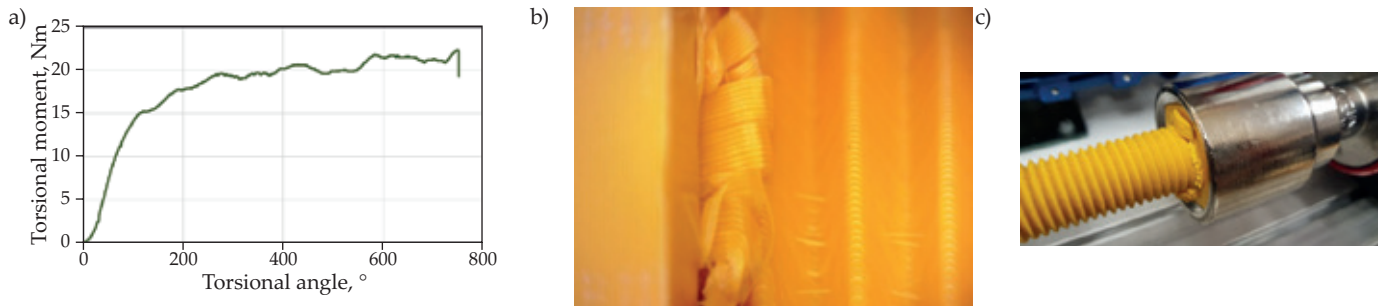

F i g . 7. PLA: a) torque vs. angle diagram, b) fracture surface morphology, c) view of the sample after testing
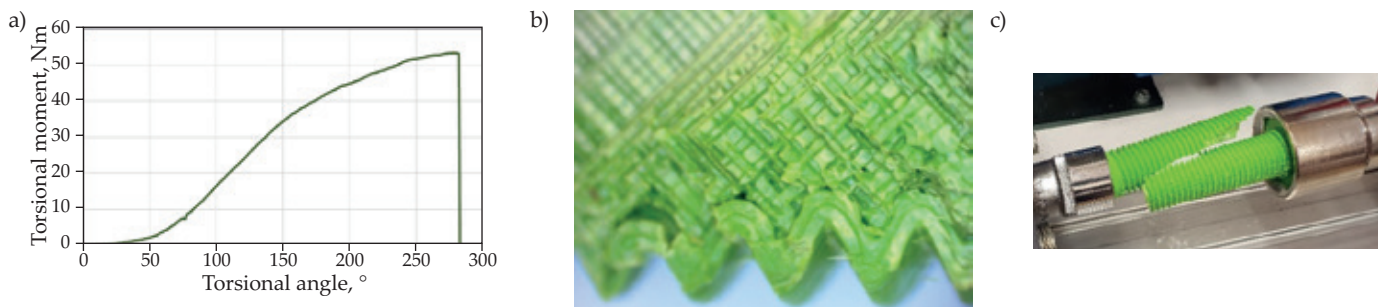

F i g. 8. ABS: a) torque vs. angle diagram, b) fracture surface morphology, c) view of the sample after testing
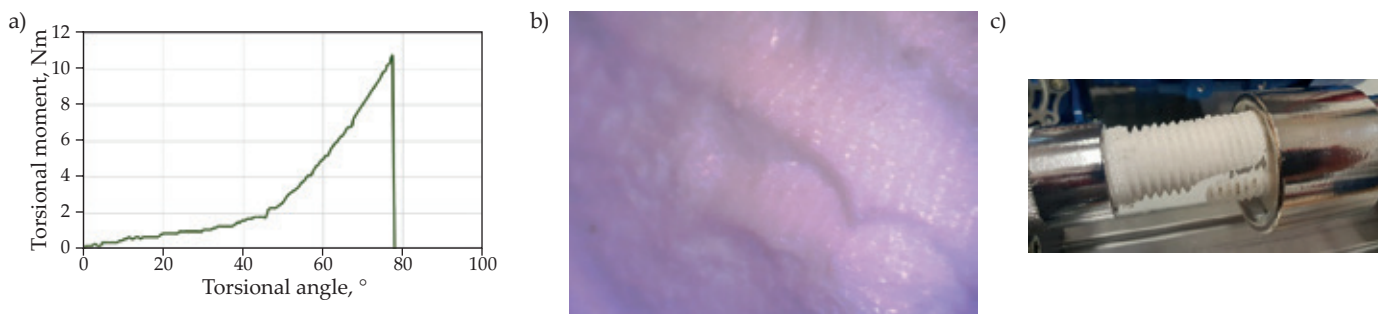

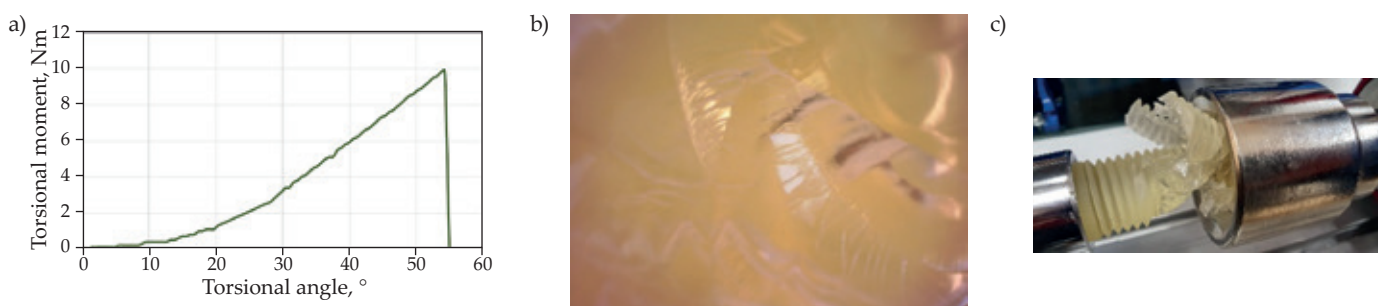**F i g. 9. PET-G: a) torque vs. angle diagram, b) fracture surface morphology, c) view of the sample after testing**

F i g. 10. RGD720: a) torque vs. angle diagram, b) fracture surface morphology, c) view of the sample after testing

T a b l e 2. **Torsional test results**

	Torsional moment, Nm									
	ABS-M30 (100)	ABS-M30 (50)	PLA (100)	PLA (50)	ABS (100)	ABS (50)	PET-G (100)	PET-G (50)	RGD720 (100)	RGD720 (50)
Sample 1	44.6	41.0	23.1	22.4	52.5	56.4	9.7	13.1	10.3	12.5
Sample 2	43.2	42.2	21.2	24.5	54.2	54.3	11.0	12	9.2	11.8
Sample 3	42.1	42.8	22.9	23	53.6	53.8	10.6	11.6	9.6	11.9
Sample 4	43.8	42.7	21.7	23.8	53.7	54.6	11.1	12.2	9.8	12.2
Sample 5	44.1	43.2	22.5	24.1	52.7	55.9	10.9	11.7	10.4	10.9
Average value	43.6	42.4	22.3	23.6	53.3	55.0	10.7	12.1	9.9	11.9
Standard deviation	1.0	0.8	0.8	0.9	0.7	1.1	0.6	0.6	0.5	0.6
Coefficient of variation	2.2	2.0	3.6	3.6	1.3	2.0	5.3	4.9	5.1	5.1

DISCUSSION

Currently, much research is carried out related to assessing dimensions - form deviations and the roughness parameters of the surface of models manufactured with additive techniques. This is due to the constant need to improve these techniques in selecting printer parameters and the use of appropriate finishing. Only a few publications on research models of threads and nuts made of polymeric materials can be found in the literature. There are mainly studies on thread measurement made with Powder Bed Fusion methods. Due to the continuous development of new types of polymeric materials, the knowledge presented in the publications can significantly improve the material extrusion techniques for the production of screw thread-nut elements. The same applies to the approach to the development of the 3D-CAD models geometry. This complex issue cannot be directly implemented basing on the guidelines provided for standard screw thread manufacturing procedures. In connection with the specificity of additive techniques, the materials used, and the manufacturing process parameters, this relationship translates into preparing the appropriate geometry of the output models. In this case, it is necessary to prepare numerical models that will ensure the correct geometry of the final products and thus the correct operation of the screw-threaded joint.

The strength tests focused mainly on the strength of the bolt. In order to increase the mechanical properties of the
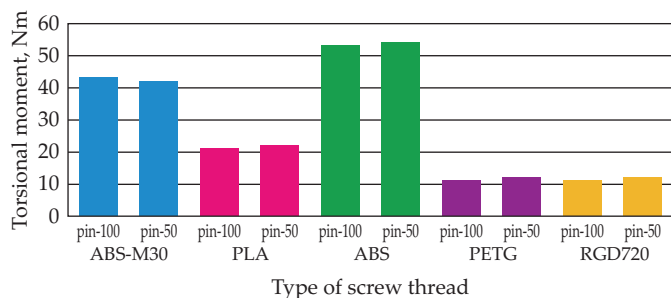

Fig. 11. Torsional moment depending on the material used and the length of the sample

screw thread, it was printed in a horizontal position. The nut was treated in the tests as an element of restraint. By analyzing the results obtained in the static torsion test and the morphology of the obtained fractures, it can be seen that the strength of threaded samples depends mainly on the type of polymer material used. The list of the transmitted torque maximum values depending on the material used and the length of the research model presented in Figure 7 shows that the samples made of ABS and ABS-M30 copolymer had the highest torsional strength. It should be noted that the value of the maximum torque for the RGD720 photopolymer resin and PET-G amorphous thermoplastic is inversely proportional to the cylindrical section samples. The results of our previous research [48–50] indicate that polymeric materials with the properties of elastic-brittle bodies are characterized by higher torsional strength than polymers such as ABS. The distribution of results can be explained by analyzing the geometry of models intended for research. On the additional supporting surface blocking the rotation of the nut, there is a cut resulting from the exit of the thread, on which, after tightening the nut, a crack appears, propagating the destruction of the sample and thus reducing its strength. There was no significant influence of the length of the sample concerning its strength.

The course of the dependence curves of the twisting moment from the torsion angle for samples made of ABS and ABS-M30 copolymer testifies to the characteristics of elastic-plastic material. In the first case, the curves have an inflection characteristic of plastic bodies with permanent plastic deformation under stress. The mean torque value was approximately 54 Nm. For samples made of ABS-M30, a yield point of about 43 Nm can be observed in the range of the torsion angle 180–200°. The yield point is not so clear due to the non-uniformity of stress distribution in the cross-section of the sample (plastic deformation first appears in the outer layer samples).

In the case of a sample made of ABS and ABS-M30 copolymer, it can be stated that the orientation of the model in the working chamber of the device has a significant impact on the decohesion nature of the obtained

fracture. The fracture analysis shows that the layers are separated gradually, and therefore the crack propagation is directly related to the way the model is filled - the alternating arrangement of the paths at 45° and 135° angles. The green, rough surface and the separation of the layers indicate a plastic fracture of the sample, consistent with the results from the tests carried out in the static torsion test.The threaded samples made of RGD720 resin and PET-G thermoplastic had the lowest torsional strength of about 11 Nm. On the basis of the torsion test results, the behavior of the samples as an elastic-brittle body was observed. The samples shown in Figure 6, after the torsion tests, had clear brittle fractures, devoid of clear traces of plastic deformation, which confirms the course of the torsion curves. We do not observe cell layers sliding apart. Subsequently, samples made of polylactide were tested. In this case, it may be surprising that the samples loaded with the torque did not deteriorate. The nut threaded a counter surface in the rotating screw thread. Two factors influenced this behavior of the sample: high plasticity of the polylactide used in the tests and modification of the screw thread geometry concerning the nominal value by assumed values of clearance, which allowed the accumulation of chips in the formed filament in the cap.

CONCLUSIONS

Additive processes allow almost any manufacturing of screw-threaded joint elements. However, it requires knowledge of the geometrical relationships of a thread itself and the strength of materials from which the screw-threaded joint is made. Thanks to the research models development and conducting tests related to dimensional accuracy and surface roughness, it is possible to test the printed models made of ABS-M30, PLA, ABS, PET-G, and RGD720 polymers in terms of strength properties.

The presented analysis of bolt strength allows to get an idea to what extent the loading of a metric bolt with axial force affects the stresses arising in it. The permissible bolt loads take into account both the strength properties of the bolt material and its geometric features, which for metric threads may be related to the bolt's outer diameter and nut height or the length of the bolt inserted into another structural element (Eqs. 13, 5, 8, 16, 17, 22). In the case of screws made of plastic with additive techniques, the inherent discontinuity of the screw material, resulting from micropores or the adoption of light internal structures, *e.g.* using different hatch patterns or scanning strategies, must also be taken into account. Moreover, the influence of the friction process of the threads surface of the bolt and nut as well as the effect of heat emitted in this process should be taken into account to a greater extent than in the case of metal materials. This is due to significantly different friction coefficients and different thermal conductivity of structural elements made of metal and plastic materials in many cases of friction pairs.

Due to the complexity of the issue, the presented research is only a starting point for further studies, which will concern, among other things, an extension of the strength tests and the presentation of additional tests taking into account new polymeric materials studies.

REFERENCES

[1] Boboulos M.: "CAD-CAM and Rapid Prototyping Application Evaluation", PhD and Ventus Publishing Aps, 2010.
[2] Gdula M.: *Metals* **2020**, *10*, 932.
https://doi.org/10.3390/met10070932
[3] Xiao W. *et al*.: *Robotics and Computer-Integrated Manufacturing* **2015**, *31*, 1.
https://doi.org/10.1016/j.rcim.2014.06.003
[4] Thompson M.K. *et al*.: *CIRP Annals* **2016**, *65*, 737.
https://doi.org/10.1016/j.cirp.2016.05.004
[5] Mazurkow A., Sikorska-Czupryna S.: *Advances In Manufacturing Science And Technology* **2020**, *44*, 71.
https://doi.org/10.2478/amst-2019-0013
[6] Baggi E.: *Adv EngSoftw* **2009**, *40*, 407.
https://doi.org/10.1016/j.advengsoft.2008.07.003
[7] Leal R., Barreiros F.M., Alves L. *et al*.: *International Journal of Advanced Manufacturing Technology* **2017**, *92*, 1671.
https://doi.org/10.1007/s00170-017-0239-8
[8] Lecklider T.: *Evaluation Engineering* **2017**, *56*, 16.
[9] Rokicki P. *et al*.: *Aircraft Engineering and Aerospace Technology. An International Journal* **2016**, *88*, 374.
https://doi.org/10.1108/aeat-01-2015-0018
[10] Raja V., Kiran J.F: "Reverse Engineering An Industrial Perspective", Springer, New York, NY, USA, 2010.
[11] Ciocca L. *et al*.: *Medical and Biological Engineering and Computing* **2012**, *50*, 743.
https://doi.org/10.1007/s11517-012-0898-4
[12] Turek P. *et al*.: *Polimery* **2020**, *65*, 510.
https://doi.org/10.14314/polimery.2020.7.2
[13] Garcia-Garcia R., Gonzalez-Palacios M.A.: *The International Journal of Advanced Manufacturing Technology* **2018**, *98*, 645.
https://doi.org/10.1007/s00170-018-2246-9
[14] Dziubek T., Oleksy M.: *Polimery* **2017**, *62*, 44.
https://doi.org/10.14314/polimery.2017.044
[15] Budzik G., Przeszlowski Ł., Wieczorowski M. *et al*.: *AIP Conference Proceedings* **2018**, 140005.
https://doi.org/10.1063/1.5034997
[16] Zhong X. *et al*.: *Engineering Structures* **2019**, *182*, 153.
https://doi.org/10.1016/j.engstruct.2018.12.065
[17] Ivanov A.S. *et al*.: *Russian Engineering Research* **2015**, *35*, 571.

https://doi.org/10.3103/s1068798x15080067

[18] Bhonge P.S., Foster B.D., Lankarani H.M.: *ASME International Mechanical Engineering Congress and Exposition* **2011**, 73.
https://doi.org/10.1115/imece2011-62905

[19] ISO 965-1:1998: ISO general purpose metric screw threads – Tolerances – Part 1: Principles and basic data, 1998.

[20] ISO 262:1998, ISO general purpose metric screw threads – Selected sizes for screws, bolts and nuts, 1998.

[21] ISO 724:1993, ISO general purpose metric screw threads – Basic dimensions, 1993.

[22] ISO 68-1:1998, ISO general purpose screw threads – Basic profile – Part 1: Metric screw threads, 1998.

[23] Leach R. K., Bourell D., Carmignato S. *et al*.: *CIRP Annals* **2019**, *68*, 677.
https://doi.org/10.1016/j.cirp.2019.05.004

[24] Kechagias, J.; Stavropoulos, P.; Koutsomichalis, A. *et al.*: *Advances in Engineering Mechanics and Materials* **2014**, 61 (accessed on 10 December 2020).
http://inase.org/library/2014/santorini/bypaper/MECHANICS/MECHANICS-07.pdf

[25] Chen L., Lin W.-S., Polido W.D. *et al.*: *Journal of Prosthetic Dentistry* **2019**, *122*, 309.
https://doi.org/10.1016/j.prosdent.2019.02.007

[26] Turek P., Budzik G., Przeszłowski Ł.: *Polymers* **2020**, *12*, 2444.
https://doi.org/10.3390/polym12112444

[27] Gibson I., Rosen D.W., Stucker B.: "Additive Manufacturing Technologies", Springer, New York, USA, 2014.

[28] Budzik G., Woźniak J., Paszkiewicz A. *et al.*: *Materials* **2021**, *14*, 2202.
https://doi.org/10.3390/ma14092202

[29] Kozior T., Adamczak S.: "Amplitude Surface Texture Parameters of Models Manufactured by FDM Technology". In The International Symposium for Production Research, Springer: Cham, Switzerland, 2018, pp. 208–217.
https://doi.org/10.1007/978-3-319-92267-6_17

[30] Fox J.C., Moylan S.P., Lane B.M.: *Procedia CIRP* **2016**, *45*, 131.
https://doi.org/10.1016/j.procir.2016.02.347

[31] Jamshidinia M., Kovacevic R.: *Surface Topography: Metrology and Properties* **2015**, *3*, 014003.
https://doi.org/10.1088/2051-672x/3/1/014003

[32] Turner B.N., Gold S.A.: *Rapid Prototyping Journal* **2015**, *21*, 250.
https://doi.org/10.1108/rpj-02-2013-0017

[33] Kawalec A., Magdziak M.: *Measurement* **2012**, *45*, 2330.
https://doi.org/10.1016/j.measurement.2011.09.022

[34] Pinto J. M., Arrieta C., Andia M.E. *et al.*: *Medical Engineering and Physics* **2015**, *37*, 328.
https://doi.org/10.1016/j.medengphy.2015.01.009

[35] Turek P., Budzik G., Sęp J. *et al.*: *Polymers* **2020**, *12*, 3029.
https://doi.org/10.3390/polym12123029

[36] Saqib S., Urbanic J.: "An experimental study to determine geometric and dimensional accuracy impact factors for fused deposition modelled parts" in "Enabling manufacturing competitiveness and economic sustainability", Springer, Berlin, Heidelberg, 2012, pp. 293-298.

[37] Pisula J., Dziubek T., Przeszłowski Ł.: *Machine Dynamics Research* **2016**, *40*, 147.
http://mdr.simr.pw.edu.pl/index.php/MDR/article/view/200/182

[38] Turek P., Budzik G.: *Polymers* **2021**, *13(14)*, 2271.
https://doi.org/10.3390/polym13142271

[39] Brajlih T., Tasic T., Drstvensek I. *et al.*: *Strojniškivestnik-Journal of Mechanical Engineering* **2011**, *57*, 826-833.
https://doi.org/10.5545/sv-jme.2010.152

[40] Bazan A., Turek P., Przeszłowski Ł.: *Journal of Mechanical Science and Technology* **2021**, *35*, 1167-1176.
https://doi.org/10.1007/s12206-021-0230-z

[41] Michaud M.: "CATIA Core Tools: Computer Aided Three-Dimensional Interactive Application", McGraw-Hill Education, 2012.

[42] ISO 4288:2011: Geometrical Product Specifications (GPS) – Surface texture: Profile method – Rules and procedures for the assessment of surface texture, 2011.

[43] ISO 25178-2:2012: Geometrical Product Specifications (GPS) – Surface Texture: Areal – Part 2: Terms, Definitions and Surface Texture Parameters, 2012.

[44] Bickford J.: "Handbook of Bolts and Bolted Joints", CRC Press, Boca Raton, 1998

[45] Childs T.H.C. (ed.): "Mechanical Design. Theory and Applications" (Third Edition), Butterworth-Heinemann, Oxford, 2021.

[46] Witek A., Grzejda R.: „Sposób modelowania złącza śrubowego a obciążenie robocze śruby". In „Podstawy Konstrukcji Maszyn. Kierunki Badań i Rozwoju". Tom III, Wyd. Politechniki Gdańskiej, Gdańsk, 2011, pp. 101-109.

[47] Witek A.: "Wytrzymałość śruby – wysokość nakrętki" (access 2021.10.29).
https://docer.pl/doc/xves588

[48] Dębski M., Magniszewski M., Bernaczek J. *et al.*: *Polimery* **2021**, *66*, 298.
https://doi.org/10.14314/polimery.2021.5.3

[49] Budzik G., Magniszewski M., Przeszłowski Ł. *et al.*: *Polimery* **2018**, *63*, 830.
https://doi.org/10.14314/polimery.2018.11.13

[50] Oleksy M. Oliwa R., Bulanda K. *et al.*: *Polimery* **2021**, *66(1)*, 52.
https://doi.org/10.14314/polimery.2021.1.7

[51] Bączkowski M., Marciniak D., Bieliński M.: *Polimery* **2021**, *66(9)*, 480.
https://doi.org/10.14314/polimery.2021.9.5

[52] Czyżewski P., Marciniak D., Nowinka B. *et al.*: *Polymers* **2022**, *14(2)*, 356.
https://doi.org/10.3390/polym14020356